THE JOURNAL OF BIOLOGICAL CHEMISTRY VOL. 286, NO. 37, pp. 32170–32177, September 16, 2011

Calpain Protects the Heart from Hemodynamic Stress*

Received for publication, April 6, 2011, and in revised form, June 22, 2011 Published, JBC Papers in Press, July 27, 2011, DOI 10.1074/jbc.M111.248088

Manabu Taneike[‡1], Isamu Mizote[‡1], Takashi Morita[‡], Tetsuya Watanabe[‡], Shungo Hikoso[‡], Osamu Yamaguchi[‡], Toshihiro Takeda[‡], Takafumi Oka[‡], Takahito Tamai[‡], Jota Oyabu[‡], Tomokazu Murakawa[‡], Hiroyuki Nakayama[§], Kazuhiko Nishida[‡], Junji Takeda[¶], Naoki Mochizuki[‖], Issei Komuro[‡], and Kinya Otsu[‡2]

From the Departments of [‡]Cardiovascular Medicine and [¶]Social and Environmental Medicine, Graduate School of Medicine, and [§]Department of Clinical Pharmacology and Pharmacogenomics, Graduate School of Pharmaceutical Sciences, Osaka University, Suita, Osaka 565-0871 and the [‖]Department of Cell Biology, National Cerebral and Cardiovascular Center Research Institute, Suita, Osaka 565-8565, Japan

Calpains make up a family of Ca^{2+}-dependent intracellular cysteine proteases that include ubiquitously expressed μ- and m-calpains. Both are heterodimers consisting of a distinct large catalytic subunit (calpain 1 for μ-calpain and calpain 2 for m-calpain) and a common regulatory subunit (calpain 4). The physiological roles of calpain remain unclear in the organs, including the heart, but it has been suggested that calpain is activated by Ca^{2+} overload in diseased hearts, resulting in cardiac dysfunction. In this study, cardiac-specific calpain 4-deficient mice were generated to elucidate the role of calpain in the heart in response to hemodynamic stress. Cardiac-specific deletion of calpain 4 resulted in decreased protein levels of calpains 1 and 2 and showed no cardiac phenotypes under base-line conditions but caused left ventricle dilatation, contractile dysfunction, and heart failure with interstitial fibrosis 1 week after pressure overload. Pressure-overloaded calpain 4-deficient hearts took up a membrane-impermeant dye, Evans blue, indicating plasma membrane disruption. Membrane repair assays using a two-photon laser-scanning microscope revealed that calpain 4-deficient cardiomyocytes failed to reseal a plasma membrane that had been disrupted by laser irradiation. Thus, the data indicate that calpain protects the heart from hemodynamic stresses, such as pressure overload.

Calpains are a family of neutral Ca^{2+}-activated cysteine proteases that are believed to participate in basic Ca^{2+}-mediated intracellular processes (1, 2). There are 14 calpain gene family members in mammals. Two ubiquitous forms of calpains have been identified, μ- and m-calpains, which are activated by micromolar and millimolar Ca^{2+} concentrations, respectively. Both are heterodimers consisting of an 80-kDa catalytic subunit (calpain 1 for μ-calpain and calpain 2 for m-calpain, which are encoded by the *Capn1* and *Capn2* genes, respectively) and a common 28-kDa regulatory subunit (calpain 4/CAPNS1 (calpain small-1), which is encoded by the *Capns1* gene).

Limited proteolysis of specific substrate proteins by calpain in distinct subcellular locations leads to their altered function in cells, and this makes calpain an important regulator of cellular signaling mechanisms (1, 2). The *in vivo* physiological function of calpain remains to be elucidated, although many potential substrate proteins have been identified. Loss-of-function studies in mice have been performed to determine the physiological functions of μ- and m-calpains (3–7). Homozygous deletion of *Capns1* abolishes the expression and activity of both μ- and m-calpains, resulting in embryonic lethality with apparent defects in the cardiovascular system and erythropoiesis (3, 6, 8). Disruption of *Capn2* also results in pre-implantation embryonic lethality (5). Thus, calpain is essential for embryonic development.

Mouse embryonic fibroblasts derived from calpain 4-deficient mice have been used to study functions of calpain *in vitro*. These studies indicate that calpains play important roles in cell migration, actin cytoskeleton organization, apoptosis, autophagy, plasma membrane repair, and membrane blebbing (9–14).

Calpain activity is increased in a wide variety of pathological conditions associated with Ca^{2+} overload (15). In the heart, increased calpain activation has been observed in pressure-overloaded myocardium, and attenuation of calpain activation by its inhibitor was found to improve contractile function (16, 17). Similarly, calpain activation and cleavage of its substrate have been reported during ischemic preconditioning and myocardial infarction (18–22), and some of these events are accompanied by programmed cell death and necrosis. These data imply a detrimental role of calpain in the diseased heart. However, loss of myocardial calpain activity by forced expression of calpastatin, an endogenous inhibitor of calpain, results in progressive dilated cardiomyopathy (23). Previously reported studies relied on small molecule inhibitors that lack complete calpain sensitivity, on overexpression of calpain or calpastatin, or on *in vitro* proteolysis of the putative calpain substrates. In this study, cardiac-specific calpain 4-deficient mice were generated to elucidate the role of calpain in the heart in response to pressure overload. This is the first report to identify an *in vivo* role of the ubiquitous calpains in the stress response.

EXPERIMENTAL PROCEDURES

Generation of Cardiac-specific Calpain 4-deficient Mice—This study was carried out under the supervision of the Animal Research Committee of Osaka University and in accordance with the Guidelines for Animal Experiments of Osaka University and the Japanese Act on Welfare and Management of Ani-

* This work was supported by a grant-in-aid for scientific research from the Ministry of Education, Culture, Sports, Science, and Technology.

[1] Both authors contributed equally to this work.

[2] To whom correspondence should be addressed: Dept. of Cardiovascular Medicine, Graduate School of Medicine, Osaka University, 2-2 Yamadaoka, Suita, Osaka 565-0871, Japan. Tel.: 81-6-6879-3632; Fax: 81-6-6879-3634; E-mail: kotsu@medone.med.osaka-u.ac.jp.

mals (No. 105). A 9.3-kb SalI-SacI fragment that included exons 1–9 from the mouse 129/SvJ genomic library was used for the targeting construct. The targeting construct was developed by inserting the *loxP* site into the SpeI site located 813 bp upstream from exon 7 and *loxP* sites along with the *PGK-neo* gene into the BamHI site located 176 bp downstream from exon 9. The targeting vector contained 7.5 kb of the homologous DNA upstream from the *loxP-PGK-neo-loxP* cassette site and 1.8 kb of the homologous DNA downstream from the third *loxP* site. PCR, Southern blotting, and karyotyping analyses were performed to obtain embryonic stem clones exhibiting the desired homologous recombination and normal karyotype. Highly chimeric mice, generated by aggregating these targeted embryonic stem cells into BDF_1 blastocysts, were bred with C57B/6J mice. To remove the selection marker gene, *PGK-neo*, and to obtain a type II deletion, F_1 mice with germ line transmission of the *loxP*-targeted *Capns1* allele were cross-bred with EIIa-*Cre* mice, resulting in heterozygous *Capns1*-floxed mice without *PGK-neo*. *α-MHCCre* mice in the C57B/6J background (24) were mated with *Capns1*-floxed mice. Primers used for PCR screening were H1F (5′-AGAGAATACATTGCAGGATAGG-3′) and H2R (5′-TATAATGAGATCTGGTGGCCTC-3′) (700-bp PCR product) and primers 246F (5′-CGTCTAAGAA-ACCATTATTATCATGAC-3′) and 246R (5′-ATGGCCAGT-ACTAGTGAACCTCTTCGA-3′) (170-bp PCR product when *PGK-neo* was floxed out).

Transverse Aortic Constriction, Echocardiography, Hemodynamic Analysis, and Drug Administration—Transverse aortic constriction (TAC)[3] operation and hemodynamic measurements were performed as described previously (25). To perform echocardiography on awakened mice, ultrasonography (SONOS-5500, equipped with a 15-MHz linear transducer, Philips Medical Systems) was used. Noninvasive measurements of blood pressure were carried out on mice anesthetized with 2.5% Avertin (26). Osmotic minipumps (ALZET Model 1002) were used to administer isoproterenol at a dose of 50 mg/kg of body weight for 2 weeks.

Histological Analysis—Hematoxylin/eosin or Azan-Mallory staining was performed on paraffin-embedded sections. The cross-sectional areas of cardiomyocytes were determined as described previously (25). The fibrotic area of the total area was assessed by computer-aided image analysis of Azan-Mallory-stained tissue sections. Three fields at 100-fold magnification for each mouse ($n = 3$) were captured and assessed. To detect apoptotic cells, triple staining with terminal deoxynucleotidyltransferase-mediated dUTP nick end labeling (TUNEL), propidium iodide, and anti-α-sarcomeric actin antibody (Sigma) was performed on paraffin-embedded sections (25). Mice were injected intraperitoneally with Evans blue dye (1 mg of dye/0.1 ml of PBS/10 g of body weight) 3 h before TAC operation. Twenty-four h after TAC, serial frozen sections of cardiac muscle were studied for dye uptake (27).

Southern and Western Blot Analyses—Southern blot analysis of embryonic stem cells or mouse hearts was performed as reported previously (25). Genomic DNA was isolated from mouse hearts, digested with PstI, and subjected to Southern blot analysis (see Fig. 2*B*). The probe used was an 892-bp PCR fragment containing exons 4–6. Protein homogenates were subjected to Western blot analysis using antibodies against calpains 1, 2, and 4 (Abcam).

Membrane Repair Assay—The *in vitro* membrane assay was performed on adult cardiomyocytes isolated from 10-week-old mice with some modifications (12). The isolated cardiomyocytes (28) were imaged using a two-photon confocal laser-scanning microscope (Olympus FV100MPE) and subjected to laser wounding at 37 °C in Tyrode's solution containing 140 mM NaCl, 5 mM KCl, 1 mM $MgCl_2$, 10 mM Hepes (pH 7.0), and 10 mM glucose in the presence of 4 μM FM® 1-43FX dye (Invitrogen) and 100 mM 2,3-butanedione monoxime (Sigma) with 1 mM Ca^{2+}. A 5-μm diameter half-circle area of the surface cardiomyocytes was irradiated with a 720-nm laser at 10% of maximum power for 300 ms. Intracellular Ca^{2+} was measured using a Fluo-4 direct calcium assay kit (Invitrogen). Calcium measurements were performed with excitation at 473 nm and fluorescence emission at 520 nm. The background fluorescence was subtracted off-line, and fluorescence (F) was normalized to the fluorescence before laser injury (F_0) and reported as F/F_0. The *in situ* membrane repair assay (27) was conducted on the whole heart with some modifications. The whole heart was placed in Tyrode's solution in the presence of 2 μM FM 1-43FX dye and 100 mM 2,3-butanedione monoxime with 1 mM Ca^{2+}. To induce membrane damage, a 5 × 200-μm rectangular area of the heart was irradiated with a 720-nm laser at maximum power at 30 μm from the surface for 500 ms. Images at 30 μm from the surface of the heart were obtained with a two-photon confocal laser-scanning microscope.

Statistics—Results are expressed as the mean ± S.E. Statistical analyses were performed using Statcel2 software (OMS Publishing Inc., Tokorozawa, Japan). Comparisons between two groups were performed using Student's t test. One-way analysis of variance with Bonferroni post hoc test was used for multiple comparisons. $p < 0.05$ was considered statistically significant.

RESULTS

Generation of Mice Lacking Calpain 4 in the Heart—To obtain cardiac-specific calpain 4-deficient mice, the *Capns1* gene was conditionally inactivated by inserting *loxP* sites in introns 6 and 9 (Fig. 1*A*). Selection cassettes comprising a neomycin resistance gene (*neo*) for positive selection and a diphtheria toxin gene for negative selection were positioned between two *loxP* sites downstream from the floxed exons and at the 3′-end of the targeting vector, respectively. Mice that harbored the *Capns1*-floxed allele and the phosphoglycerate kinase *PGK-neo* cassette selection marker gene were crossed with EIIa-*Cre* mice to obtain heterozygous *Capns1*-floxed mice without the *PGK-neo* cassette (29). The homozygous *Capns1*-floxed mice ($Capns1^{flox/flox}$) appeared normal and were externally indistinguishable from littermates of other genotypes. To disrupt the *Capns1* gene selectively in the myocardium, $Capns1^{flox/flox}$ mice were crossed with mice expressing the *Cre* recombinase under the control of the α-myosin heavy chain

[3] The abbreviations used are: TAC, transverse aortic constriction; TUNEL, terminal deoxynucleotidyltransferase-mediated dUTP nick end labeling; LV, left ventricle.

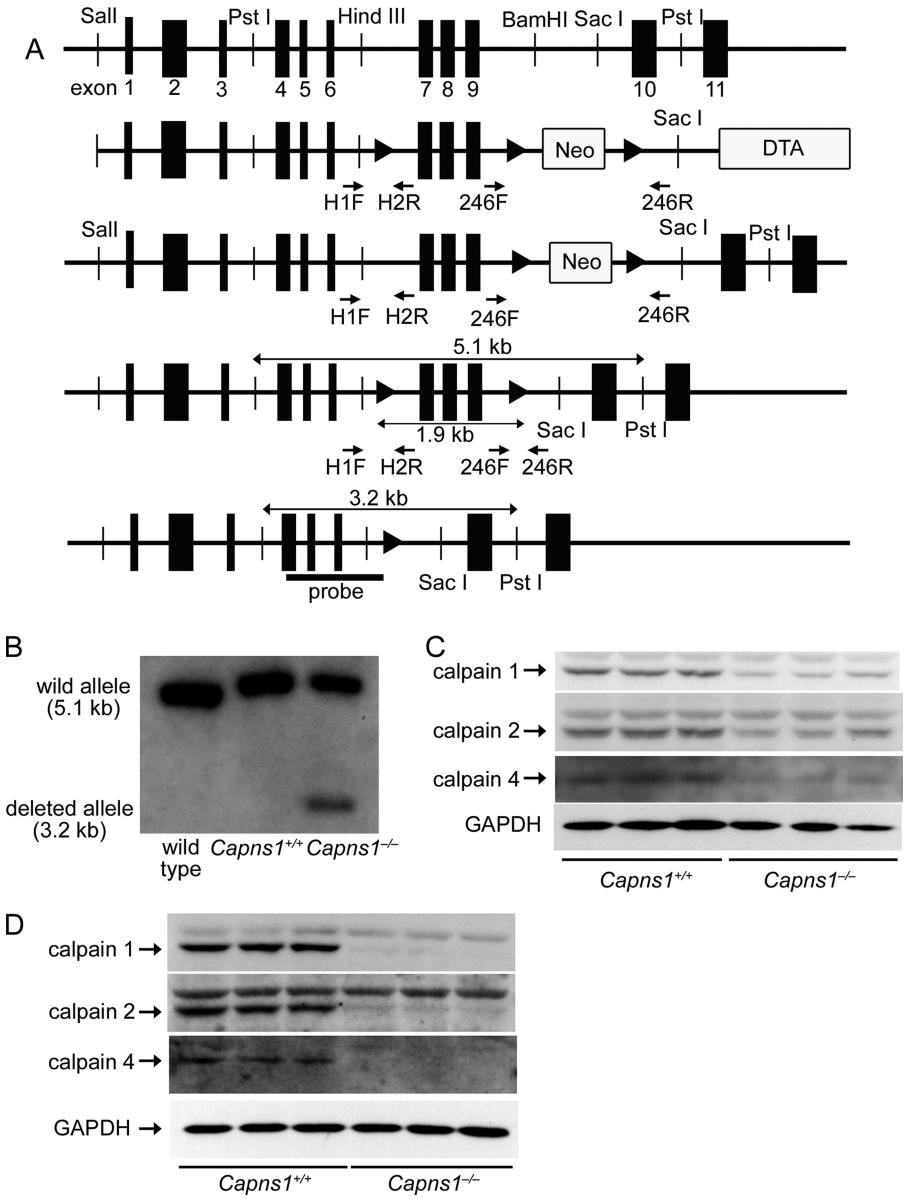

FIGURE 1. **Targeted modification of the *Capns1* gene.** *A*, schematic structures of genomic *Capns1* sequences, the targeting construct, the targeted allele, the type II deletion, and the *Capns1*$^{-/-}$ allele (from *top* to *bottom*). The *arrowheads* represent *loxP* sites. The targeting construct includes the *PGK-neo* cassette flanked by *loxP* sites and a diphtheria toxin gene (*DTA*). The *arrows* correspond to the primer sequences for PCR screening. The *bar* labeled *probe* corresponds to the sequence used for Southern blotting analysis in *B*. *B*, genomic analysis of *in vivo* hearts. Genomic DNA was isolated from mouse hearts, digested with PstI, and analyzed by Southern blotting with the probe. *C* and *D*, protein expression of the calpain family in whole heart homogenates (*C*) and in partially purified adult cardiomyocytes (*D*) from 10-week-old mice.

promoter (*α-MHCCre* mice) (24) to obtain *Capns1*$^{flox/flox}$:*α-MHCCre*$^{+}$ mice (*Capns1*$^{-/-}$). *Capns1*$^{flox/flox}$:*α-MHCCre*$^{-}$ littermates (*Capns1*$^{+/+}$) were used as controls. Southern blot analysis of the mouse hearts indicated successful recombination in *Capns1*$^{flox/flox}$:*α-MHCCre*$^{+}$ hearts (Fig. 1*B*). Immunoblotting revealed an ~77% reduction of calpain 4 protein in the *Capns1*$^{-/-}$ hearts (Fig. 1*C*). When adult cardiomyocytes were isolated as a partially purified single cell preparation, calpain 4 protein in *Capns1*$^{-/-}$ cardiomyocytes was not detected. In *Capns1*$^{-/-}$ mice, 50 and 31% reductions were observed in the levels of calpains 1 and 2, respectively, in whole heart homogenates and ~96 and 80% reductions in the levels of calpains 1 and 2, respectively, in a partially purified adult cardiomyocyte preparation (Fig. 1*D*). These results agree with previous reports that demonstrated that ablation of *Capns1* results in a loss of calpain 1 and 2 proteins (3, 6, 8).

Normal Cardiac Structure and Function in Calpain 4-deficient Mice—Capns1$^{-/-}$ and *Capns1*$^{+/+}$ mice were born at the expected Mendelian ratio of 48:52, respectively. *Capns1*$^{-/-}$ mice were normal at birth, and their external appearance was indistinguishable from that of their littermates. The mice grew to adulthood and were fertile. There was no difference in survival at 1 year between *Capns1*$^{-/-}$ and *Capns1*$^{+/+}$ mice. *Capns1*$^{-/-}$ hearts showed no evidence of cardiac morphological defects. Histological examination of hearts from 10-week-old *Capns1*$^{-/-}$ mice revealed no myofibrillar disarray, necrosis, or fibrosis (data not shown). Physiological and echocardiographic parameters were not significantly different between

TABLE 1

Physiological, echocardiographic, and hemodynamic parameters in *Capns1*$^{+/+}$ and *Capns1*$^{-/-}$ mice at base line

Data are expressed as the mean ± S.E. There were no significant differences between *Capns1*$^{+/+}$ and *Capns1*$^{-/-}$ mice in any parameters. IVSd, diastolic interventricle septum wall thickness; LVIDd, end-diastolic LV internal dimension; LVIDs, end-systolic LV internal dimension; LVPWd, diastolic LV posterior wall thickness; LVFS, LV fractional shortening.

	Capns1$^{+/+}$ (n = 8)	*Capns1*$^{-/-}$ (n = 9)
Body weight (g)	24.7 ± 0.7	24.3 ± 0.5
Tibia length (mm)	18.0 ± 0.1	17.9 ± 0.1
Heart weight (mg)	111.5 ± 2.4	113.1 ± 3.0
Lung weight (mg)	127.0 ± 3.8	129.6 ± 3.0
Heart weight/body weight (mg/g)	4.52 ± 0.11	4.66 ± 0.09
Lung weight/body weight (mg/g)	5.14 ± 0.10	5.35 ± 0.14
	Capns1$^{+/+}$ (n = 10)	*Capns1*$^{-/-}$ (n = 10)
IVSd (mm)	0.77 ± 0.08	0.79 ± 0.08
LVIDd (mm)	2.66 ± 0.03	2.73 ± 0.03
LVIDs (mm)	1.36 ± 0.11	1.35 ± 0.05
LVPWd (mm)	0.77 ± 0.02	0.77 ± 0.02
LVFS (%)	48.9 ± 1.0	50.5 ± 0.4
Heart rate (/min)	664.8 ± 17.0	655.5 ± 22.5

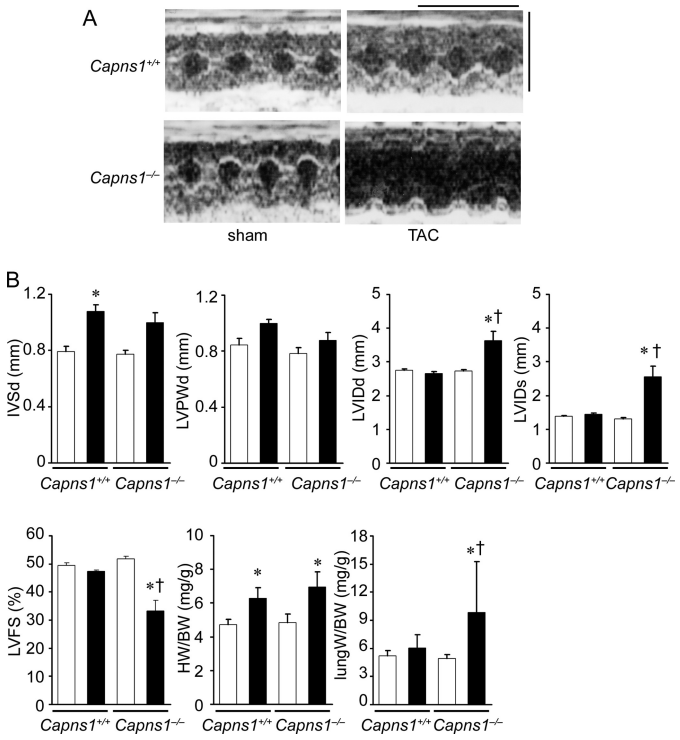

FIGURE 2. **Development of cardiomyopathy in *Capns1*$^{-/-}$ mice in response to pressure overload.** *Capns1*$^{-/-}$ mice were analyzed 7 days after TAC. *A*, representative M-mode echocardiographic tracings. *Scale bars* = 0.2 s and 5 mm, respectively. *B*, echocardiographic and physiological parameters. *Open* and *closed bars* represent sham- and TAC-operated groups, respectively. Sham-operated *Capns1*$^{+/+}$ mice (n = 7), TAC-operated *Capns1*$^{+/+}$ mice (n = 12), sham-operated *Capns1*$^{-/-}$ mice (n = 8), and TAC-operated *Capns1*$^{-/-}$ mice (n = 13) are shown. Values are expressed as the mean ± S.E. *, $p < 0.05$ *versus* the corresponding sham-operated group; †, $p < 0.05$ *versus* TAC-operated *Capns1*$^{+/+}$ mice. *IVSd*, diastolic interventricle septum wall thickness; *LVPWd*, diastolic LV posterior wall thickness; *LVIDd*, end-diastolic LV internal dimension; *LVIDs*, end-systolic LV internal dimension; *LVFS*, LV fractional shortening; *HW*, heart weight; *BW*, body weight.

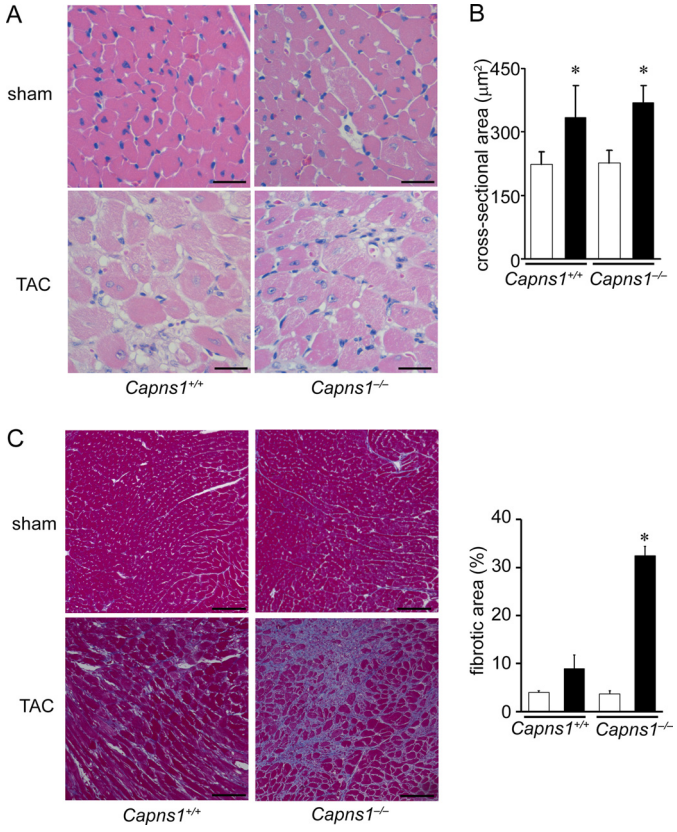

FIGURE 3. **Histological analysis of *Capns1*$^{-/-}$ hearts 7 days after TAC.** *A*, hematoxylin/eosin-stained heart sections. *Scale bars* = 25 μm. *B*, cardiomyocyte cross-sectional area measured in the sections in *A*. *Open* and *closed bars* represent sham- and TAC-operated groups, respectively. Values are expressed as the mean ± S.E. *, $p < 0.05$ *versus* the corresponding sham-operated group. *C*, Azan-Mallory-stained heart sections. Quantification of fibrotic area is shown in the *graph*. *Scale bars* = 100 μm. *Open* and *closed bars* represent sham- and TAC-operated groups, respectively. Values are expressed as the mean ± S.E. *, $p < 0.05$ *versus* all other groups.

Capns1$^{-/-}$ and *Capns1*$^{+/+}$ mice (Table 1). Thus, *Capns1*$^{-/-}$ mice had normal global cardiac structure and function.

Development of Congestive Heart Failure in Response to Pressure Overload in Calpain 4-deficient Mice—Ten-week-old *Capns1*$^{-/-}$ and *Capns1*$^{+/+}$ mice were subjected to TAC. In wild-type mice, pressure overload by TAC induced cardiac hypertrophy without any signs of contractile dysfunction 1 week after the operation and heart failure 4 weeks after the operation (25). One week after TAC, echocardiographic analysis was performed (Fig. 2, *A* and *B*). One week after sham operation, the end-diastolic and end-systolic left ventricle (LV) internal dimensions and LV fractional shortening, an index of contractility, were not significantly different between *Capns1*$^{-/-}$ and *Capns1*$^{+/+}$ mice. However, end-diastolic and end-systolic LV internal dimensions were significantly elevated, and LV fractional shortening was significantly reduced in TAC-operated *Capns1*$^{-/-}$ mice compared with both sham-operated *Capns1*$^{-/-}$ and TAC-operated *Capns1*$^{+/+}$ mice (Fig. 2*B*). Furthermore, the lung/body weight ratio, an index of lung congestion, was significantly elevated in TAC-operated *Capns1*$^{-/-}$ mice compared with the other groups. These findings indicate that *Capns1*$^{-/-}$mice develop congestive heart failure in response to pressure overload.

Although TAC increased the heart/body weight ratio and cardiomyocyte cross-sectional area in both *Capns1*$^{-/-}$ and *Capns1*$^{+/+}$ mice, there was no significant difference between the two groups (Figs. 2*B* and 3, *A* and *B*). Thus, calpain is not related to pressure overload-induced cardiac hypertrophy. Azan-Mallory staining revealed interstitial and perivascular fibrosis in both TAC-operated *Capns1*$^{-/-}$ and *Capns1*$^{+/+}$

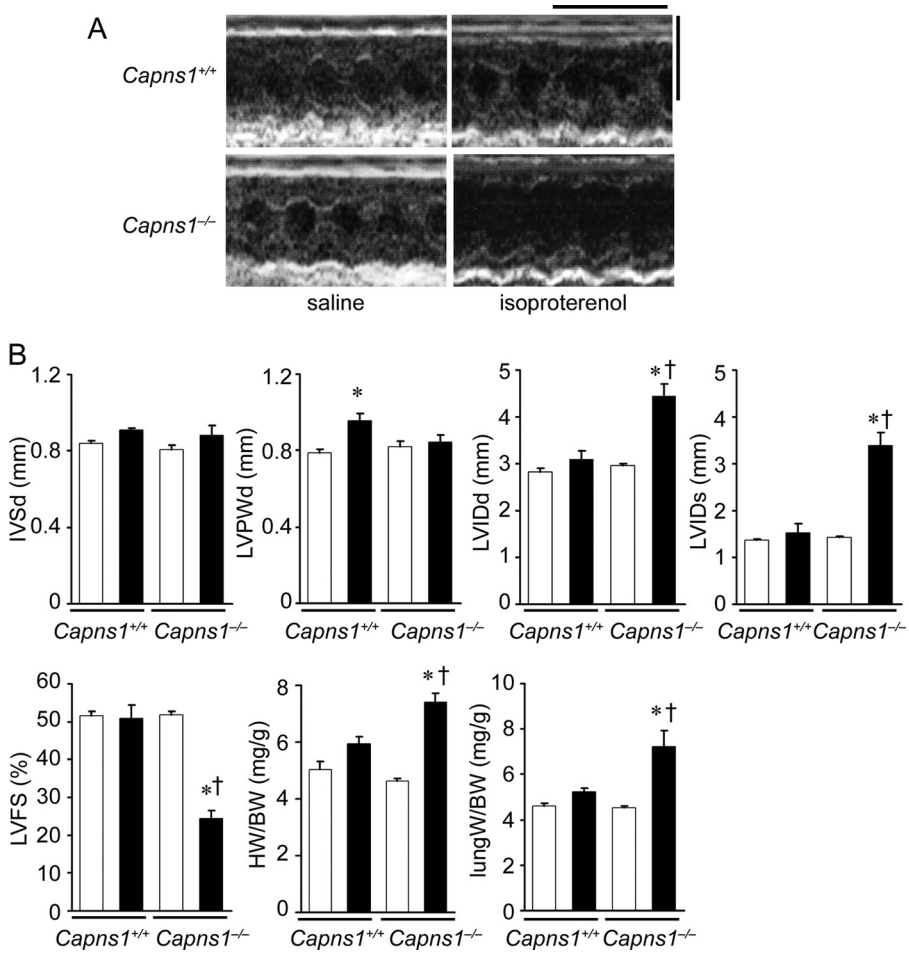

FIGURE 4. **β-Adrenergic stress-induced cardiac dysfunction in *Capns1*$^{-/-}$ mice.** Isoproterenol or saline was administered to *Capns1*$^{-/-}$ and *Capns1*$^{+/+}$ mice for 2 weeks. *A*, representative images of transthoracic M-mode echocardiographic tracing 2 weeks after an infusion of isoproterenol. *Scale bars* = 0.2 s and 5 mm, respectively. *B*, echocardiographic and physiological parameters. Values are expressed as the mean ± S.E. ($n = 4$ in each group). *Open* and *closed bars* represent saline- and isoproterenol-treated groups, respectively. *, $p < 0.05$ *versus* the corresponding saline-treated group; †, $p < 0.05$ *versus* isoproterenol-treated *Capns1*$^{+/+}$ mice. *IVSd*, diastolic interventricle septum wall thickness; *LVPWd*, diastolic LV posterior wall thickness; *LVIDd*, end-diastolic LV internal dimension; LVIDs, end-systolic LV internal dimension; *LVFS*, LV fractional shortening; *HW*, heart weight; *BW*, body weight.

hearts, but the extent of fibrosis in *Capns1*$^{-/-}$ mice was greater than in *Capns1*$^{+/+}$ mice (Fig. 3*C*).

To confirm that calpain protects the heart against external stress, the role of calpain was examined in β-adrenergic stimulation-induced cardiac remodeling. Because β-adrenergic hyperactivation is observed in failing hearts, the isoproterenol infusion model has been employed to elucidate molecular mechanisms underlying cardiac remodeling (28). Isoproterenol infusion for 2 weeks induced LV chamber dilatation and cardiac dysfunction in *Capns1*$^{-/-}$ mice but not in *Capns1*$^{+/+}$ mice (Fig. 4). Thus, calpain has a protective role in response to external stresses such as pressure overload and β-adrenergic stimulation.

Defective Membrane Repair in Calpain 4-deficient Hearts—In this study, we attempted to elucidate the molecular mechanism underlying the beneficial role of calpain against pressure overload. Calpain exists in the cytosol as an inactive form, translocates to membranes, and is activated at the membrane in response to increases in cellular calcium (2, 30, 31). First, the structural stability of the sarcolemma was tested by examining Evans blue dye uptake into TAC-operated *Capns1*$^{-/-}$ hearts. In *Capns1*$^{-/-}$ mice, sporadic Evans blue dye-positive cardiomyocytes were observed 24 h after TAC. This was not the case with hearts from TAC-operated *Capns1*$^{+/+}$ or sham-operated *Capns1*$^{-/-}$ mice (Fig. 5, *A* and *B*).

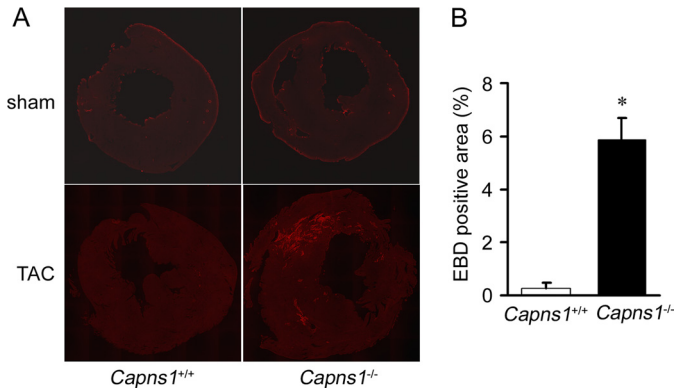

FIGURE 5. **Plasma membrane damage in *Capns1*$^{-/-}$ hearts.** *A*, uptake of Evans blue dye in the hearts of *Capns1*$^{-/-}$ and *Capns1*$^{+/+}$ mice following TAC or sham operation. *B*, Evans blue dye (*EBD*)-positive area per LV cross-sectional area in TAC-operated *Capns1*$^{-/-}$ ($n = 6$) and *Capns1*$^{+/+}$ ($n = 4$) mice. Values are expressed as the mean ± S.E. *, $p < 0.05$.

Hemodynamic stress can cause membrane damage by two different mechanisms: enhanced susceptibility to the stress and

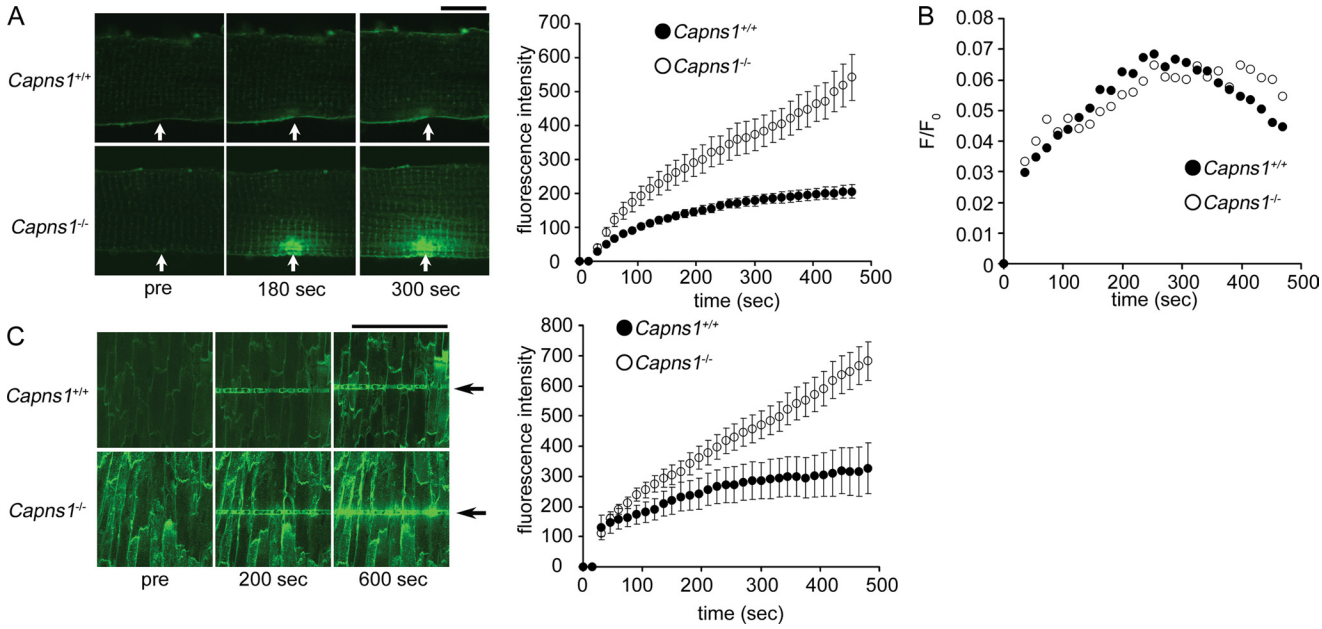

FIGURE 6. **Impaired plasma membrane repair in *Capns1*$^{-/-}$ cardiomyocytes.** *A*, time course of membrane sealing after laser injury in isolated cardiomyocytes. *Capns1*$^{-/-}$ and *Capns1*$^{+/+}$ cardiomyocytes were injured with a pulsed laser in the presence of FM 1-43FX with 1 mM Ca^{2+}. *Left panel*, representative images; *right panel*, fluorescence *versus* time ($n = 12–14$). *Scale bar* = 10 μm. *Arrows* indicate laser damage. *B*, time course of Fluo-4 fluorescence during the resealing process. *Capns1*$^{-/-}$ and *Capns1*$^{+/+}$ cardiomyocytes were loaded with Fluo-4 and injured with a pulsed laser with 1 mM Ca^{2+}. The background fluorescence was subtracted off-line, and fluorescence (*F*) was normalized to the fluorescence before laser injury (F_0) and reported as F/F_0. F/F_0 *versus* time is shown. *C*, hearts from *Capns1*$^{-/-}$ and *Capns1*$^{+/+}$ mice were damaged with a linear laser in the presence of FM 1-43FX with 1 mM Ca^{2+}. Images at 30 μm from the surface of the heart were obtained. *Left panel*, representative images 0 (*pre*), 200, and 600 s after laser irradiation; *right panel*, fluorescence *versus* time ($n = 3$). *Scale bar* = 100 μm. *Arrows* indicate laser damage.

defective membrane repair. To visualize real-time sealing in injured cardiomyocytes, a laser-based assay was used to measure resealing kinetics in adult cardiomyocytes isolated from *Capns1*$^{-/-}$ mice (12). In this assay, staining of internal membranes by an otherwise membrane-impermeable dye, FM 1-43FX, was monitored microscopically over time after laser disruption. Resealing blocked further dye entry through the disruption and halted cell staining. Therefore, the measured whole cell fluorescence reached a plateau upon the completion of resealing. Although the *Capns1*$^{+/+}$ cardiomyocytes resealed within 250 s, the *Capns1*$^{-/-}$ cardiomyocytes continued to take up FM 1-43FX dye for at least 480 s (Fig. 6*A*). These results indicate that membrane resealing was impaired in the *Capns1*$^{-/-}$ cardiomyocytes. When the intracellular Ca^{2+} concentration was measured using the Ca^{2+}-sensitive fluorescent dye Fluo-4, an increase in the fluorescent signal was detected at the position of laser exposure. The time course of Fluo-4 fluorescence during the resealing process was similar for *Capns1*$^{-/-}$ and *Capns1*$^{+/+}$ cardiomyocytes, but *Capns1*$^{+/+}$ cardiomyocytes tended to show lower fluorescence intensity compared with *Capns1*$^{-/-}$ mice thereafter (Fig. 6*B*). The power of laser irradiation was varied to estimate its threshold for detection of the staining of internal membranes. There was no significant difference in the minimum level of laser power (6% of maximum laser power) to detect membrane damage between *Capns1*$^{-/-}$ and *Capns1*$^{+/+}$ cardiomyocytes.

To confirm impaired membrane repair in *Capns1*$^{-/-}$ cardiomyocytes, an *in situ* membrane repair assay was performed on the surface cardiomyocytes of the heart (27). The membranes of cardiomyocytes were wounded by maximum power irradiation with an infrared laser in the presence of FM 1-43FX dye. Images were obtained at 30 μm from the surface of the heart. After laser injury, the FM 1-43FX fluorescence intensity initially increased but halted within 100–150 s in *Capns1*$^{+/+}$ hearts, whereas the fluorescence intensity continuously increased in *Capns1*$^{-/-}$ hearts (Fig. 6*C*). Although a subtle effect of calpain deletion on membrane fragility cannot be ruled out, the impaired membrane repair would lead to enhanced susceptibility to stress in *Capns1*$^{-/-}$ mice.

DISCUSSION

In this study, we generated cardiac-specific calpain 4-deficient mice to elucidate a role of calpain in the heart. Because ablation of *Capns1* results in a loss of calpain 1 and 2 proteins (3, 6, 8), calpain 4-deficient mice or cells have been used to study functions of μ- and m-calpains. We have shown that *Capns1*$^{-/-}$ mice had normal global cardiac structure and function, indicating that the ubiquitous calpain in cardiomyocytes is not essential for cardiac development in mice. Homozygous deletion of *Capns1* results in embryonic lethality with apparent defects in the cardiovascular system (3, 6, 8). Therefore, calpain in non-cardiomyocytes appears to play an important role in the development of the cardiovascular system, or the residual non-floxed-out cardiomyocytes contribute to normal cardiac development.

Furthermore, calpain was shown to play a beneficial role in response to hemodynamic stress. The cardioprotective role of calpain was confirmed by the experiment showing that a β-adrenergic stimulant induced LV chamber dilatation and cardiac dysfunction in *Capns1*$^{-/-}$ mice. This is the first report to identify the *in vivo* role of the ubiquitous calpains in the stress response using a loss-of-function technique. The data from this

study are not in agreement with previous work from other laboratories that demonstrated that calpain causes the alteration of a number of specific proteins, leading to subcellular remodeling and cardiac dysfunction (17, 32–34). This discrepancy may be caused by the use of non-selective calpain inhibitors or a non-physiological substrate. However, calpain reportedly promotes both apoptosis and survival signals in response to different cell death stimuli (10). Further investigation will be necessary to elucidate the role of calpain regarding cell death in other experimental models such as ischemia-reperfusion.

In vitro studies using *Capns1*$^{-/-}$ cells indicate that the protective roles of calpain come from regulation of apoptosis, autophagy, proliferation, actin cytoskeleton organization, and focal adhesion or membrane repair (7, 9–12, 14). The anti-apoptotic role of calpain has been reported (10, 14). In fact, a 3-fold increase was observed in the number of TUNEL-positive cardiomyocytes in TAC-operated *Capns1*$^{-/-}$ hearts (data not shown). Although the anti-apoptotic effect of calpain may contribute to the observed phenotypes in TAC-operated *Capns1*$^{-/-}$ hearts, the level of apoptosis in *Capns1*$^{-/-}$ hearts appears to be too low to develop cardiomyopathy within 1 week of TAC (35). We have reported previously that autophagy protects the heart from hemodynamic stress (28). However, in this study, we did not see a significant suppression of autophagic activity in TAC-operated *Capns1*$^{-/-}$ hearts as estimated by Western blotting of LC3, which is a molecular marker for autophagy. Furthermore, sarcomere disorganization in *Capns1*$^{-/-}$ hearts was not observed. Because cardiomyocytes are terminally differentiated cells, proliferation or differentiation does not seem to be involved in the protective function of calpain. In this study, we showed that the structural stability of the plasma membrane was reduced in TAC-operated *Capns1*$^{-/-}$ hearts and that membrane resealing was impaired in the isolated *Capns1*$^{-/-}$ cardiomyocytes. The sustained membrane damage could cause cardiomyocyte loss and replacement fibrosis in TAC-operated *Capns1*$^{-/-}$ hearts. However, the possibility that a mechanism other than impaired membrane repair is responsible for the development of cardiomyopathy in *Capns1*$^{-/-}$ hearts cannot be excluded.

The mechanism of membrane resealing is now well characterized at the cellular level. A large plasma membrane disruption elicits Ca^{2+}-activated homotypic vesicle fusion locally and rapidly. The "patch" vesicles thus formed then fuse exocytotically with the plasma membrane surrounding the defect site, restoring barrier continuity (36, 37). Removal of the actin cytoskeleton at the damaged area of the plasma membrane is a critical early event for resealing. Although identification of the protein components of this process is under way, several candidate repair proteins have been identified, including vesicle SNARE (soluble NSF attachment protein receptor) and target SNARE (38), dysferlin (27, 39), annexin A1 (40), and calpain (12). Dysferlin-deficient mice show significant Evans blue uptake in cardiomyocytes, impaired sarcolemma repair, and cardiomyopathy after stress exercise, similar to what was observed in *Capns1*$^{-/-}$ hearts in response to pressure overload. This supports the original hypothesis that calpain is involved in plasma membrane repair in pressure-overloaded hearts. Calpain activity is required for cytoskeletal remodeling after membrane disruption (12). Removal of the damaged actin network mediated through calpain activation may serve to prepare the wound area for subsequent events that initiate restoration of the cytoskeleton and membrane sealing. The exact role of calpain in the membrane repair process should be investigated.

In conclusion, this study provides clear evidence that calpain protects the heart from hemodynamic stress. The results suggest the need to reassess the rationale for the application of calpain inhibitors as therapeutic agents to prevent pathological activation of calpain in heart failure.

Acknowledgments—We thank Prof. Alan Wells (University of Pittsburgh) for calpain 2 cDNA and Kana Takada for technical assistance.

REFERENCES

1. Goll, D. E., Thompson, V. F., Li, H., Wei, W., and Cong, J. (2003) *Physiol. Rev.* **83,** 731–801
2. Suzuki, K., Hata, S., Kawabata, Y., and Sorimachi, H. (2004) *Diabetes* **53,** S12–S18
3. Arthur, J. S., Elce, J. S., Hegadorn, C., Williams, K., and Greer, P. A. (2000) *Mol. Cell. Biol.* **20,** 4474–4481
4. Azam, M., Andrabi, S. S., Sahr, K. E., Kamath, L., Kuliopulos, A., and Chishti, A. H. (2001) *Mol. Cell. Biol.* **21,** 2213–2220
5. Dutt, P., Croall, D. E., Arthur, J. S., Veyra, T. D., Williams, K., Elce, J. S., and Greer, P. A. (2006) *BMC Dev. Biol.* **6,** 3
6. Zimmerman, U. J., Boring, L., Pak, J. H., Mukerjee, N., and Wang, K. K. (2000) *IUBMB Life* **50,** 63–68
7. Shimada, M., Greer, P. A., McMahon, A. P., Bouxsein, M. L., and Schipani, E. (2008) *J. Biol. Chem.* **283,** 21002–21010
8. Tan, Y., Dourdin, N., Wu, C., De Veyra, T., Elce, J. S., and Greer, P. A. (2006) *Genesis* **44,** 297–303
9. Dourdin, N., Bhatt, A. K., Dutt, P., Greer, P. A., Arthur, J. S., Elce, J. S., and Huttenlocher, A. (2001) *J. Biol. Chem.* **276,** 48382–48388
10. Tan, Y., Wu, C., De Veyra, T., and Greer, P. A. (2006) *J. Biol. Chem.* **281,** 17689–17698
11. Demarchi, F., Bertoli, C., Copetti, T., Tanida, I., Brancolini, C., Eskelinen, E. L., and Schneider, C. (2006) *J. Cell Biol.* **175,** 595–605
12. Mellgren, R. L., Zhang, W., Miyake, K., and McNeil, P. L. (2007) *J. Biol. Chem.* **282,** 2567–2575
13. Larsen, A. K., Lametsch, R., Elce, J., Larsen, J. K., Thomsen, B., Larsen, M. R., Lawson, M. A., Greer, P. A., and Ertbjerg, P. (2008) *Biochem. J.* **411,** 657–666
14. Bertoli, C., Copetti, T., Lam, E. W., Demarchi, F., and Schneider, C. (2009) *Oncogene* **28,** 721–733
15. Huang, Y., and Wang, K. K. (2001) *Trends Mol. Med.* **7,** 355–362
16. Greyson, C. R., Schwartz, G. G., Lu, L., Ye, S., Helmke, S., Xu, Y., and Ahmad, H. (2008) *J. Mol. Cell. Cardiol.* **44,** 59–68
17. Mani, S. K., Shiraishi, H., Balasubramanian, S., Yamane, K., Chellaiah, M., Cooper, G., Banik, N., Zile, M. R., and Kuppuswamy, D. (2008) *Am. J. Physiol. Heart Circ. Physiol.* **295,** H314–H326
18. Iwamoto, H., Miura, T., Okamura, T., Shirakawa, K., Iwatate, M., Kawamura, S., Tatsuno, H., Ikeda, Y., and Matsuzaki, M. (1999) *J. Cardiovasc. Pharmacol.* **33,** 580–586
19. Papp, Z., van der Velden, J., and Stienen, G. J. (2000) *Cardiovasc. Res.* **45,** 981–993
20. Chen, M., Won, D. J., Krajewski, S., and Gottlieb, R. A. (2002) *J. Biol. Chem.* **277,** 29181–29186
21. Singh, R. B., Chohan, P. K., Dhalla, N. S., and Netticadan, T. (2004) *J. Mol. Cell. Cardiol.* **37,** 101–110
22. Khalil, P. N., Neuhof, C., Huss, R., Pollhammer, M., Khalil, M. N., Neuhof, H., Fritz, H., and Siebeck, M. (2005) *Eur. J. Pharmacol.* **528,** 124–131
23. Galvez, A. S., Diwan, A., Odley, A. M., Hahn, H. S., Osinska, H., Melendez, J. G., Robbins, J., Lynch, R. A., Marreez, Y., and Dorn, G. W., 2nd (2007) *Circ. Res.* **100,** 1071–1078
24. Yamaguchi, O., Watanabe, T., Nishida, K., Kashiwase, K., Higuchi, Y.,

Takeda, T., Hikoso, S., Hirotani, S., Asahi, M., Taniike, M., Nakai, A., Tsujimoto, I., Matsumura, Y., Miyazaki, J., Chien, K. R., Matsuzawa, A., Sadamitsu, C., Ichijo, H., Baccarini, M., Hori, M., and Otsu, K. (2004) *J. Clin. Invest.* **114,** 937–943
25. Nishida, K., Yamaguchi, O., Hirotani, S., Hikoso, S., Higuchi, Y., Watanabe, T., Takeda, T., Osuka, S., Morita, T., Kondoh, G., Uno, Y., Kashiwase, K., Taniike, M., Nakai, A., Matsumura, Y., Miyazaki, J., Sudo, T., Hongo, K., Kusakari, Y., Kurihara, S., Chien, K. R., Takeda, J., Hori, M., and Otsu, K. (2004) *Mol. Cell. Biol.* **24,** 10611–10620
26. Hikoso, S., Yamaguchi, O., Nakano, Y., Takeda, T., Omiya, S., Mizote, I., Taneike, M., Oka, T., Tamai, T., Oyabu, J., Uno, Y., Matsumura, Y., Nishida, K., Suzuki, K., Kogo, M., Hori, M., and Otsu, K. (2009) *Circ. Res.* **105,** 70–79
27. Han, R., Bansal, D., Miyake, K., Muniz, V. P., Weiss, R. M., McNeil, P. L., and Campbell, K. P. (2007) *J. Clin. Invest.* **117,** 1805–1813
28. Nakai, A., Yamaguchi, O., Takeda, T., Higuchi, Y., Hikoso, S., Taniike, M., Omiya, S., Mizote, I., Matsumura, Y., Asahi, M., Nishida, K., Hori, M., Mizushima, N., and Otsu, K. (2007) *Nat. Med.* **13,** 619–624
29. Lakso, M., Pichel, J. G., Gorman, J. R., Sauer, B., Okamoto, Y., Lee, E., Alt, F. W., and Westphal, H. (1996) *Proc. Natl. Acad. Sci. U.S.A.* **93,** 5860–5865
30. Molinari, M., and Carafoli, E. (1997) *J. Membr. Biol.* **156,** 1–8
31. Shao, H., Chou, J., Baty, C. J., Burke, N. A., Watkins, S. C., Stolz, D. B., and Wells, A. (2006) *Mol. Cell. Biol.* **26,** 5481–5496
32. Gao, W. D., Atar, D., Liu, Y., Perez, N. G., Murphy, A. M., and Marban, E. (1997) *Circ. Res.* **80,** 393–399
33. Tsuji, T., Ohga, Y., Yoshikawa, Y., Sakata, S., Abe, T., Tabayashi, N., Kobayashi, S., Kohzuki, H., Yoshida, K. I., Suga, H., Kitamura, S., Taniguchi, S., and Takaki, M. (2001) *Am. J. Physiol. Heart Circ. Physiol.* **281,** H1286–H1294
34. Suryakumar, G., Kasiganesan, H., Balasubramanian, S., and Kuppuswamy, D. (2010) *J. Cardiovasc. Pharmacol.* **55,** 567–573
35. Wencker, D., Chandra, M., Nguyen, K., Miao, W., Garantziotis, S., Factor, S. M., Shirani, J., Armstrong, R. C., and Kitsis, R. N. (2003) *J. Clin. Invest.* **111,** 1497–1504
36. McNeil, P. L., and Terasaki, M. (2001) *Nat. Cell Biol.* **3,** E124–E129
37. McNeil, P. L., and Steinhardt, R. A. (2003) *Annu. Rev. Cell Dev. Biol.* **19,** 697–731
38. Bi, G. Q., Alderton, J. M., and Steinhardt, R. A. (1995) *J. Cell Biol.* **131,** 1747–1758
39. Bansal, D., Miyake, K., Vogel, S. S., Groh, S., Chen, C. C., Williamson, R., McNeil, P. L., and Campbell, K. P. (2003) *Nature* **423,** 168–172
40. McNeil, A. K., Rescher, U., Gerke, V., and McNeil, P. L. (2006) *J. Biol. Chem.* **281,** 35202–35207